

# FINE-GRAINED FORECASTING MODELS VIA GAUSSIAN PROCESS BLURRING EFFECT

Sepideh Koohfar & Laura Dietz

Department of Computer Science

University of New Hampshire

Durham, NH 03820, USA

{Sepideh.Koohfar, Laura.Dietz}@usnh.edu

## ABSTRACT

Time series forecasting is a challenging task due to the existence of complex and dynamic temporal dependencies. This can lead to incorrect predictions by even the best forecasting models. Using more training data is one way to improve the accuracy, but this source is often limited. In contrast, we are building on successful denoising approaches for image generation by advocating for an end-to-end forecasting and denoising paradigm.

We propose an end-to-end forecast-blur-denoise forecasting framework by encouraging a division of labors between the forecasting and the denoising models. The initial forecasting model is directed to focus on accurately predicting the coarse-grained behavior, while the denoiser model focuses on capturing the fine-grained behavior that is locally blurred by integrating a Gaussian Process model. All three parts are interacting for the best end-to-end performance. Our extensive experiments demonstrate that our proposed approach is able to improve the forecasting accuracy of several state-of-the-art forecasting models as well as several other denoising approaches. The code for reproducing our main result is open-sourced and available online.<sup>1</sup>

## 1 INTRODUCTION

Time series forecasting is a vital foundational technology in many important domains such as in economics Capistrán et al. (2010), health care Lim (2018), demand forecasting Salinas et al. (2020) and autonomous driving Chang et al. (2019). Despite the recent advances in neural networks, time series forecasting still remains a challenging problem. The complexity and dynamic nature of temporal dependencies across different time scales pose a challenge for forecasting models to accurately replicate the temporal patterns

Denoising models Ho et al. (2020) have recently gained popularity in generating high quality images. Typically denoising models Vincent et al. (2010) are trained to reverse an image corrupting process, thereby learning correlation patterns of the application domain. Including weak supervision via a denoising objective will train models to simultaneously predict and denoise, resulting in more resilient models overall.

In this work, we rethink ideas from variational denoising models in applications to time series forecasting task, which is defined as follows:

**Time series forecasting task.** Given  $\kappa$  time series observations prior to cutoff a time step  $t_0$ , the task is to predict values of the target variable  $\gamma$  for the next  $\tau$  time steps into the future (from  $t_0$  to  $t_0 + \tau$ ). We refer to the given time series as  $X = \{\mathbf{x}_t; \gamma_t\}_{t=t_0-\kappa}^{t_0}$ , and the to be predicted series as  $Y = \{\gamma_t\}_{t=t_0}^{t_0+\tau}$ . The target variable can be multivariate with  $\gamma_t \in \mathbb{R}^{d_y}$ , although we focus on datasets with univariate target variables ( $d_y = 1$ ). The given time series observations  $X$  include  $d_x$  covariates, such as season or time of day. Additionally, each observation  $X_t$  encompasses the target variable  $\gamma_t$  prior to time step  $t_0$ , yielding  $X_t \in \mathbb{R}^{d_x+d_y}$ .

<sup>1</sup>Code available at <https://github.com/SepKfr/Fine-grained-Gaussian-Process-Forecasting>

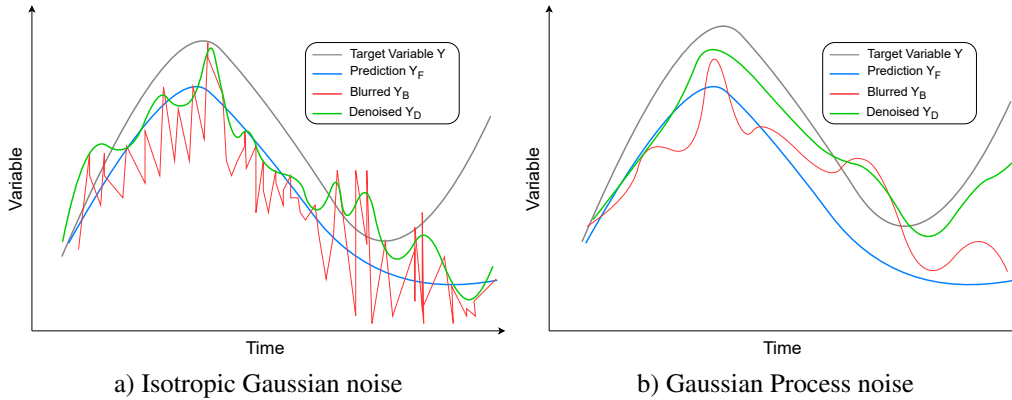


Figure 1: A synthetic example of blurring and denoising the prediction. The left figure a) illustrates that blurring and denoising the prediction with isotropic Gaussian noise results in less desirable forecasts, where the denoising model attempts to remove the jitters. However, as depicted in the right figure b) blurring and denoising the prediction with GP model results in a smooth behavior with improved fine-grained details.

**Idea.** Inspired by the success of denoising models in generating high quality images by reverting a noise process, our approach involves constructing fine-grained forecasting models. We propose a novel forecasting and denoising framework, presenting a forecast-blur-denoise framework. We envision for an intermediate blur model, strategically dividing the responsibilities of forecasting and denoising models by locally blurring the initial forecasts. We posit that this division of tasks guides the forecasting model to concentrate on accurately predicting broad and coarse-grained behavior. Simultaneously, the denoising model is focused on predicting fine-grained details by eliminating the introduced blur. Based on the division of tasks, we introduce our proposed framework as the forecast(broad)-blur-denoise(detailed) forecasting model. Hence, in this paper, we use the terms “forecast-blur-denoise” and “broad-blur-detailed” interchangeably.

When applied to image generation, denoising models usually revert a corruption process of pixel-wise isotropic Gaussian noise. With applications to time series forecasting, however, the isotropic corruption process will introduce what we call *jitters* (see red function in Figure 1 left), as the noise added to one time step is independent of noise added to subsequent time steps. Since most time series exhibit smooth behavior, the result of the isotropic corruption process yields time series that are rather unnaturally behaving. Moreover, according to our preliminary experiments, most of the state-of-the-art forecasting models do not produce predictions with many jitters. Hence, we hypothesize that the benefit of isotropic noise for improving time series forecasting via our broad-blur-detailed approach is somewhat limited, as it prompts the denoising model to merely eliminate the introduced jitters.

In this work we explore alternative techniques for training denoising models for time series forecasting. As our goal is to train the denoising model to focus on accurately predicting the fine-grained details (rather than removing jitters), we are interested in an intermediate model that locally blurs the initial forecasts by generating smooth and correlated signals. Given that the isotropic Gaussian will generate jitters due to its temporally uncorrelated nature, in line with Robinson et al. (2018) we will employ a Gaussian Process as the intermediate model that naturally models correlation across time to provide smooth functions. By locally blurring the initial forecasts, we contemplate for a distinct division of tasks between the forecasting and denoising models. We hypothesize that the absence of the intermediate blurring model may result in a less pronounced division of tasks, potentially causing the denoiser to deprioritize the accurate prediction of fine-grained details, consequently deteriorating the performance. This hypothesis is supported in the experimental section.

**Related work.** Our goal is to improve the forecasting ability of the existing time series forecasting models. Among various time series forecasting models, the ones that utilize transformers have demonstrated superior performance Li et al. (2019); Fan et al. (2019). But even the state-of-the-art time series forecasting models make wrong predictions. We will apply our approach to improve two of the best forecasting models, the Autoformer and the Informer model. The Autoformer model Wu et al. (2021) improves on the basic attention mechanism by decomposing a time series into sub-series

and incorporating an auto-correlation mechanism to capture the correlation between these sub-series. This leads to gains in efficiency and accuracy. The Informer model Zhou et al. (2021) employs ProbSparse attention, which prunes the attention matrix by focusing on samples that are outliers from a uniform distribution. Both these models are included in our experimental evaluation.

Probabilistic time series forecasting models such as DeepAR Salinas et al. (2020) generate predictions by drawing samples from a learned Isotropic Gaussian distribution. These models aim to learn the parameters of the Gaussian distribution via a deep neural network model such as LSTMs Hochreiter & Schmidhuber (1997).

Denoising models often revert a corruption process applied to the input during training to increase the robustness and generalization of the model. Therefore, the performance of time series forecasting models could as well be improved when integrated with a denoising approach. One of such approaches is the TimeGrad Rasul et al. (2021) forecasting model that uses denoising diffusion models to reverse the isotropic Gaussian noise added to the input time series. TimeGrad estimates the parameters of the Gaussian distribution using recurrent neural networks architectures LSTM/GRU. However, prior works including Koochfar & Dietz (2022); Khandelwal et al. (2018) show that LSTMs do not perform competitively compared to transformer-based forecasting methods.

DLinear model proposed by Zeng et al. (2023) proposes a *navive* time series forecasting model that only uses simple multi-layer perceptrons projections from previous observations to make predictions. We compare our proposed model to DLinear model in our experimental section.

Recently, Li et al. (2022) introduce D3VAE, a novel approach that combines bidirectional variational auto-encoder techniques with diffusion, denoising, and disentanglement to enhance time series representation. However, in line with DLinear, this approach does not include sequential modeling techniques, resulting in limited competitiveness when compared to transformer-based forecasting methods.

**Contributions.** In this work, we take a different approach by enhancing the performance of forecasting models by proposing a fine-grained forecasting framework. (1) Rather than blurring the input solely during training, we advocate for an end-to-end broad-blur-detailed forecasting framework that encourages a separation of concerns for the forecasting and denoising models. (2) Our complementary approach can be readily added to a wide-range of forecasting models. (3) Our novel approach is an alternative towards approaches that use denoising solely during training or when leveraging boosting. We experimentally show that our approach predominately outperforms many of those baselines. (4) We further demonstrate that for smooth time series data, isotropic Gaussians are not a suitable corruption model.

## 2 METHODOLOGY

Time series forecasting models using a ground truth series  $Y$ , are trained to learn the expected behavior of the target variable over time. However, complex dependencies and external factors can lead to erroneous predictions. Adding more training data can help to improve the forecasting model’s performance, but it is often a limited resource. In this work we explore how ideas from denoising models can increase the generalization of the family of forecasting models.

### 2.1 BACKGROUND: ISOTROPIC DENOISING APPROACHES

Denoising models are trained to reverse a corruption process. For this purpose, true data  $X$  is corrupted with noise to obtain a corrupted version  $\tilde{X}$ . The denoising part of the model is trained to, given  $\tilde{X}$ , predict the original data  $X$ . Often this is modelled by predicting the noise, which is then subtracted from  $\tilde{X}$  to obtain the original data  $X$ . Denoising models can be trained for the iterative reversal of noise (reasoning on a series of latents with different noise level) or in single step with a conditional model  $X|\tilde{X}$  Deja et al. (2022). The denoising objective can be optimized by itself or in combination with other objectives such as prompted image generation or time series forecasts Nichol & Dhariwal (2021).

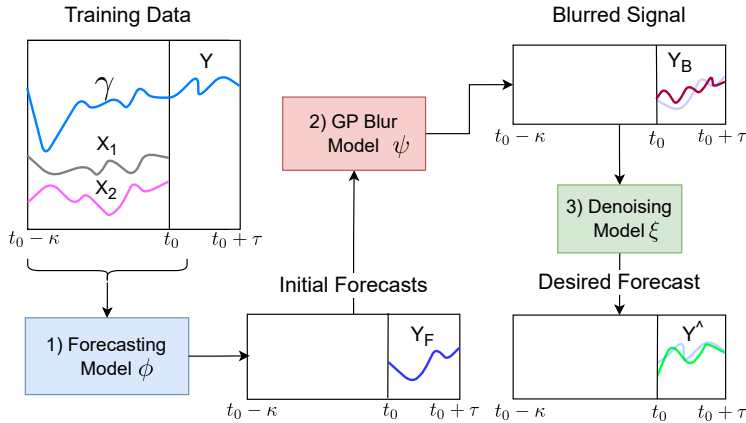


Figure 2: Our proposed model’s framework for end-to-end training the forecasting, GP blur, and denoising model. The multi-step neural network forecasting model predicts  $Y_F$  from covariates  $X_1$ ,  $X_2$ , and previous target variable  $\gamma$ . The predictions  $Y_F$  are then blurred by our GP model to obtain  $Y_B$ . The blurred predictions  $Y_B$  are then denoised by our denoising model to obtain  $Y_D = \hat{Y}$ .

Most current work uses a simple corruption process that employs an isotropic Gaussian noise model, where  $\tilde{X} \sim \mathcal{N}(\tilde{X}; X, \sigma^2 \mathbf{I})$  that acts independently on different data points, i.e., pixels for image generation Nichol & Dhariwal (2021) or time steps for time series forecasts Rasul et al. (2021).

2.2 ISSUES WITH UNCORRELATED NOISE MODELS FOR TIME SERIES

Isotropic Gaussian noise is one of the most commonly employed corruption processes, which provides noise that is identically and independently distributed (*i.i.d.*) and when used to generate observations for time series are lacking smooth behavior over time. While isotropic Gaussian noise corruption can (and are) applied to time series, the result is a corruption in the form of jitters (as depicted in red in Figure 1a). However, time series forecasting models are based on the assumption that data points are correlated over time—and hence not *i.i.d.* The effect on the training problem is that the denoiser may only learn to remove jitters. However, most errors in forecasting models are not due to jitters, as predicted forecasts are usually smooth functions that merely exhibit incorrect fine-grained behavior. In this work we go even one step further and train a smooth and correlated noise/blur model. We hypothesize that this model is more advantageous as it directs the denoising model to focus on accurately predicting the fine-grained details that are locally blurred, rather than simply eliminating jitters.

2.3 LOCALLY-BLURRED SIGNALS WITH GAUSSIAN PROCESSES

To obtain a more resilient model, we instead propose to include a noise/blur model that generates smooth temporally-correlated functions, to train the denoising model, as depicted in Figure 1b). We employ a Gaussian Process (GP) which models the correlation between consecutive samples in a sequence of observations via a kernel function  $k_\psi$ .

We generate smoothly correlated signals by drawing samples from the probability density function (PDF) of Gaussian Process (GP) denoted as  $b_\psi$ :

$$b_\psi(\tilde{X}|X) = \mathcal{N}(\tilde{X}; X, k_\psi(X, X) + \sigma^2 \mathbf{I}) \tag{1}$$

where  $\psi$  denotes the parameters of the GP kernel that are trained as part of our proposed joint model for the best end-to-end performance.

In Section 3 we will experimentally support our claim that locally blurring the initial forecasts with GPs leads to more effective training for time series forecasting than isotropic Gaussians.

2.4 BROAD-BLUR-DETAILED FORECASTING FRAMEWORK

There are many ways to exploit ideas from denoising models for time series forecasting: as separate negative training data, as a secondary objective on true time series, via auto-encoders, or as an integral part of an end-to-end model. Based on preliminary experiments, in this work we integrate ideas into a joint broad-blur-detailed forecasting model. The model integrates 1) a forecasting model, 2) an intermediate GP blurring model, and 3) a denoising model as depicted in Figure 2. All parts are jointly trained for best MSE performance. We describe these components in detail below.

- 1) Forecasting model:** Any time series forecasting model can be used here that, given the observations  $X = \{\mathbf{x}_t; \gamma_t\}_{t=t_0-\tau}^{t_0}$  predicts the future target variables  $Y_F$ , as represented by the blue box in Figure 2. We experimentally demonstrate that our end-to-end framework will help train more accurate and resilient forecasting models. We refer to the set of parameters of the forecasting model as  $\phi$ .
- 2) GP blur model:** The initial predictions  $Y_F$  are locally blurred by the GP function, depicted as a light red box in Figure 2. As described above, we suggest to use a Gaussian Process as the blur model to obtain  $Y_B \sim b_\psi(Y_B|Y_F)$ . GP parameters  $\psi$  are trained jointly with other parameters of our end-to-end forecasting and denoising model. Alternative noise models could be used here, which we explore in Section 3.
- 3) Denoising Model:** Given the locally blurred predictions  $Y_B$ , the denoising model focuses on predicting the fine-grained details by removing the blurs, which consequently improves the initial forecasting. While many architectures could be chosen for the denoising model, we choose to use the same time series forecasting model with a new set of parameters  $\xi$  as the denoiser to obtain final predictions  $Y_D = \hat{Y}$ . The denoising model is represented by the green box in Figure 2.

The result is a compound model that encourages the initial forecasting model to focus on modelling coarse-grained behavior, and a denoising model that corrects the fine-grained details. This is encouraged by an intermediate GP model that will “blur” fine-grained details in the forecast, and a denoising model that focuses on correcting these fine-grained details. Additionally, the denoising component acts as a fall-back for when the initial forecasting model fails, reducing the likelihood of catastrophic errors.

Note that for fixed training data  $X$  and  $Y$ , a new blurring effect is sampled in every epoch, deterring the model from overfitting to any particular blurring pattern.

To optimize the GP model’s parameters, we employ a strategy reminiscent of the scalable variational Gaussian Process (GP) method introduced by Hensman et al. (2015). Their scalable variational GP technique offers a computationally efficient approximation of the GP model, achieving nearly linear computational complexity for  $k_\psi(X, X)$  as the forecasting horizon increases.

2.5 END-TO-END FORECASTING AND GP LOSS

With an abundance of training data, the compound model could be trained end-to-end, predicting  $\hat{Y}$  from given  $X$  and minimizing the distance to the ground truth  $Y$  via an MSE (or  $L_2$ ) forecasting loss.

We optimize the parameters of our GP model using the ground truth  $Y$ . This allows for the efficient optimization of the parameters of variational Gaussian processes. The compound loss function employed for end-to-end training is defined as follows, where the variational evidence lower bound (ELBO) optimizes the GP model to obtain an ideal blurring effect:

$$\mathcal{L} = \underbrace{L_{\text{MSE}}}_{\text{forecasting loss}}(\hat{Y} = Y|X, Y_F, Y_B, \phi, \psi, \xi) + \lambda \underbrace{L_{\text{ELBO}}}_{\text{GP loss}}(Y_B = Y|X, Y_F, \phi, \psi) \tag{2}$$

In our experiments, following Nichol & Dhariwal (2021) we set  $\lambda$  to a small number ( $\lambda = 0.001$ ) to prevent the loss  $L_{\text{ELBO}}$  from overwhelming the  $L_{\text{MSE}}$  loss. Figure 2 illustrates our end-to-end framework.

Table 1: Overall results of the quantitative evaluation of our forecast-blur-denoise and other baseline forecasting models in terms of average and standard error of **MSE**. We compare the forecasting models on all three datasets with different number of forecasting steps. A lower **MSE** indicates a better model. Our forecast-blur-denoise approach with GPs predominantly improves performance of the original forecasting model (Autoformer) and isotropic Gaussian noise model (AutoDI). (Note that to provide a fair comparison, all the baseline models considered in this study were trained and evaluated under the *same* experimental setup as our proposed model. Consequently, the reported results may differ from those originally reported in the respective baseline papers. We provide the baseline models implementation in our online repository).

Dataset	Horizon	<b>AutoDG(Ours)</b>	Autoformer	AutoDI	NBeats	DLinear	DeepAR	CMGP	ARIMA
Traffic	24	<b>0.392</b> ±0.006	0.412 ±0.006	0.405 ±0.003	0.475 ±0.008	0.553 ±0.000	0.888 ±0.000	0.824 ±0.000	1.436 ±0.000
	48	<b>0.387</b> ±0.001	0.422 ±0.004	0.416 ±0.001	0.462 ±0.012	0.547 ±0.000	0.944 ±0.000	0.828 ±0.000	1.444 ±0.000
	72	<b>0.380</b> ±0.001	<b>0.383</b> ±0.003	0.394 ±0.002	0.465 ±0.003	0.540 ±0.000	0.877 ±0.000	0.893 ±0.000	1.459 ±0.000
	96	<b>0.385</b> ±0.003	0.400 ±0.004	0.411 ±0.002	0.464 ±0.002	0.539 ±0.000	0.860 ±0.000	0.859 ±0.000	1.444 ±0.000
Electricity	24	<b>0.165</b> ±0.001	0.187 ±0.003	0.170 ±0.001	0.200 ±0.001	0.222 ±0.000	1.039 ±0.000	1.000 ±0.000	1.707 ±0.000
	48	<b>0.188</b> ±0.003	0.203 ±0.008	0.207 ±0.003	0.218 ±0.000	0.238 ±0.000	1.014 ±0.000	0.987 ±0.000	1.729 ±0.000
	72	<b>0.209</b> ±0.004	0.230 ±0.001	0.253 ±0.004	0.234 ±0.007	0.264 ±0.000	1.023 ±0.000	0.993 ±0.000	1.759 ±0.000
	96	<b>0.211</b> ±0.001	0.230 ±0.014	0.316 ±0.002	0.237 ±0.001	0.264 ±0.000	1.013 ±0.000	0.971 ±0.000	1.747 ±0.000
Solar	24	<b>0.446</b> ±0.002	0.472 ±0.003	0.473 ±0.001	0.612 ±0.006	0.828 ±0.000	0.999 ±0.000	1.001 ±0.000	1.869 ±0.000
	48	<b>0.546</b> ±0.003	0.603 ±0.004	0.574 ±0.001	0.717 ±0.001	0.928 ±0.000	0.968 ±0.000	1.007 ±0.000	1.872 ±0.000
	72	<b>0.666</b> ±0.003	<b>0.667</b> ±0.004	0.698 ±0.002	0.766 ±0.006	0.978 ±0.000	0.974 ±0.000	1.002 ±0.000	1.855 ±0.000
	96	<b>0.713</b> ±0.004	0.739 ±0.009	0.730 ±0.005	0.827 ±0.001	1.004 ±0.000	0.974 ±0.000	0.997 ±0.000	1.874 ±0.000

### 3 EXPERIMENTS

We experimentally demonstrate the success of our forecast-corrupt-denoise approach across three datasets and two state-of-the-art forecasting models. We first focus on demonstrating the efficacy of our treatment and the importance of using correlated noise of GPs, rather than isotropic Gaussians. Next, we compare our denoising approach to a wide range of canonical denoising and ensemble baselines.

#### 3.1 EXPERIMENTAL SETUP

We lay out the conditions for our experimental evaluation.

**Datasets.** We select three widely used datasets that have been used for training and validation by a significant amount of research papers Salinas et al. (2020); Li et al. (2019); Wu et al. (2021); Zhou et al. (2021).

**Traffic**<sup>2</sup>: A univariate dataset, containing the occupancy rate ( $y_t \in [0, 1]$ ) of 440 SF Bay Area freeways, aggregated on hourly interval.

<sup>2</sup>Traffic <https://archive.ics.uci.edu/ml/machine-learning-databases/00204/PEMS-SF.zip>

Table 2: Overall results of the quantitative evaluation of our forecast-blur-denoise and other baseline forecasting models in terms of average and standard error of **MSE**. We compare the forecasting models on all three datasets with different number of forecasting steps. A lower **MSE** indicates a better model. Our forecast-blur-denoise approach with GPs predominantly improves performance of the original forecasting model (Informer) and isotropic Gaussian noise model (InfoDI). (Note that to provide a fair comparison, all the baseline models considered in this study were trained and evaluated under the *same* experimental setup as our proposed model. Consequently, the reported results may differ from those originally reported in the respective baseline papers. We provide the baseline models implementation in our online repository).

Dataset	Horizon	InfoDG(Ours)	Informer	InfoDI	NBeats	DLinear	DeepAR	CMGP	ARIMA
Traffic	24	<b>0.398</b> ±0.006	0.421 ±0.006	0.415 ±0.003	0.475 ±0.008	0.553 ±0.000	0.888 ±0.000	0.824 ±0.000	1.436 ±0.000
	48	<b>0.399</b> ±0.001	0.434 ±0.004	0.395 ±0.001	0.462 ±0.012	0.547 ±0.000	0.944 ±0.000	0.828 ±0.000	1.444 ±0.000
	72	<b>0.380</b> ±0.001	0.436 ±0.001	0.395 ±0.002	0.465 ±0.002	0.540 ±0.000	0.877 ±0.000	0.893 ±0.000	1.459 ±0.000
	96	<b>0.397</b> ±0.003	<b>0.402</b> ±0.003	<b>0.402</b> ±0.004	0.464 ±0.004	0.539 ±0.000	0.860 ±0.000	0.859 ±0.000	1.444 ±0.000
Electricity	24	<b>0.193</b> ±0.001	0.222 ±0.001	0.212 ±0.003	0.200 ±0.001	0.222 ±0.000	1.039 ±0.000	1.000 ±0.000	1.707 ±0.000
	48	<b>0.222</b> ±0.003	0.262 ±0.007	0.229 ±0.003	0.218 ±0.003	0.238 ±0.000	1.014 ±0.000	0.987 ±0.000	1.729 ±0.000
	72	<b>0.238</b> ±0.001	0.280 ±0.004	0.253 ±0.004	<b>0.234</b> ±0.007	0.264 ±0.000	1.023 ±0.000	0.993 ±0.000	1.759 ±0.000
	96	0.242 ±0.001	0.289 ±0.002	0.275 ±0.014	<b>0.237</b> ±0.001	0.264 ±0.000	1.013 ±0.000	1.130 ±0.000	1.747 ±0.000
Solar	24	<b>0.455</b> ±0.009	0.524 ±0.003	<b>0.465</b> ±0.006	0.612 ±0.006	0.828 ±0.000	0.999 ±0.000	0.971 ±0.000	1.869 ±0.000
	48	<b>0.556</b> ±0.005	0.629 ±0.003	0.570 ±0.005	0.717 ±0.001	0.928 ±0.000	0.968 ±0.000	1.007 ±0.000	1.872 ±0.000
	72	<b>0.643</b> ±0.003	0.729 ±0.023	0.707 ±0.002	0.766 ±0.006	0.978 ±0.000	0.974 ±0.000	1.002 ±0.000	1.855 ±0.000
	96	<b>0.708</b> ±0.004	0.770 ±0.004	0.766 ±0.009	0.827 ±0.005	1.004 ±0.000	0.974 ±0.000	0.997 ±0.000	1.874 ±0.000

Table 3: Comparison of different denoising baselines to our forecast-blur-denoise approach with GPs when treating Autoformer forecasting model. We find that our approach predominantly outperforms the other denoising approaches. Results are reported as average and standard error of **MSE**. A lower **MSE** indicates a better forecasting model.

Dataset	Horizon	AutoDG(Ours)	Autoformer	AutoDI	AutoDWC	AutoRB	AutoDT
Traffic	24	<b>0.392</b> ±0.006	0.412 ±0.006	0.405 ±0.003	0.400 ±0.005	0.447 ±0.006	0.430 ±0.015
	48	<b>0.387</b> ±0.001	0.422 ±0.007	0.416 ±0.007	0.417 ±0.009	0.450 ±0.005	0.410 ±0.005
	72	<b>0.380</b> ±0.001	<b>0.383</b> ±0.002	0.394 ±0.002	0.398 ±0.003	0.430 ±0.004	0.404 ±0.006
	96	<b>0.385</b> ±0.003	0.400 ±0.004	0.411 ±0.002	0.405 ±0.001	0.413 ±0.002	0.422 ±0.002
Electricity	24	<b>0.165</b> ±0.001	0.187 ±0.003	0.170 ±0.001	0.174 ±0.000	0.260 ±0.001	0.170 ±0.007
	48	<b>0.188</b> ±0.003	0.203 ±0.008	0.207 ±0.003	0.219 ±0.002	0.222 ±0.002	0.200 ±0.002
	72	<b>0.209</b> ±0.004	0.230 ±0.001	0.253 ±0.004	0.218 ±0.010	0.234 ±0.022	0.212 ±0.002
	96	<b>0.211</b> ±0.001	0.230 ±0.014	0.316 ±0.002	0.226 ±0.008	0.296 ±0.011	0.218 ±0.004
Solar	24	<b>0.446</b> ±0.002	0.472 ±0.003	0.473 ±0.006	<b>0.449</b> ±0.003	0.527 ±0.006	0.457 ±0.004
	48	<b>0.546</b> ±0.005	0.603 ±0.003	0.574 ±0.001	0.605 ±0.005	0.595 ±0.005	0.598 ±0.003
	72	<b>0.666</b> ±0.003	<b>0.667</b> ±0.004	0.698 ±0.002	0.690 ±0.010	0.718 ±0.002	0.670 ±0.006
	96	<b>0.713</b> ±0.004	0.739 ±0.009	0.730 ±0.005	0.732 ±0.006	0.753 ±0.007	0.733 ±0.006

**Solar Energy**<sup>3</sup>: A univariate dataset about solar power that could be obtained across different locations in America, collected on an hourly interval.

**Electricity**<sup>4</sup>: A univariate dataset listing the electricity consumption of 370 customers, aggregated on an hourly level.

From each dataset, we roughly use 40,000 samples, where each sample contains given observations  $X$  of  $\kappa = 192$  time steps, from which (using multiple horizon forecasting) we predict the next  $\tau \in \{24, 48, 72, 96\}$  future time steps. After Z-score normalization, we partition 40,000 samples of each dataset into three parts, 80% for training, 10% for validation, and 10% for performance evaluation.

**Evaluation metrics.** We evaluate our model and other alternatives using mean squared error  $MSE = \frac{1}{n}(\sum_{t=1}^n (y_t - \hat{y}_t)^2)$ , where  $n$  denotes the length of the predicted time series. We also study the mean absolute error  $MAE = \frac{1}{n}(\sum_{t=1}^n |y_t - \hat{y}_t|)$ , where we obtain the same findings (omitted from this manuscript, but available in Appendix A).

### 3.2 TREATED TIME SERIES FORECASTING MODELS AND BASELINES

Since our corruption-resilient approach can be used to treat any forecasting model, we study the benefit for the following state-of-the-art time series forecasting models. The number of layers is tuned with Optuna.

**Autoformer Wu et al. (2021):** A multi-layer Autoformer model with auto-correlation

**Informer Zhou et al. (2021):** A multi-layer informer with ProbAttention.

We conduct a comparative analysis focusing on the following treatments applied to the Autoformer and Informer forecasting model:

**Auto(Info)DG (our proposed model):** Our proposed forecast-blur-denoise framework with Gaussian-Process-based corruption model as described in Section 2.

**Auto(Info)DI (denoise scaled Isotropic noise):** the same forecast-corrupt-denoise model, albeit using scaled isotropic Gaussians as the noise model (instead of the GP).

**Auto(In)former (only forecasting):** the original untreated forecasting method.

We also compare against the following baselines:

**ARIMA Hyndman & Khandakar (2008):** An autoregressive integrated moving average.

**CMGP Chakrabarty et al. (2021):** Model calibration using Bayesian Optimization and GPs.

**DeepAR Salinas et al. (2020):** An Autoregressive probabilistic time series forecasting model that uses LSTMs to estimate the parameters of a Gaussian distribution.

**DLinear Zeng et al. (2023):** A forecasting model that uses multi-layer perceptron to make predictions.

**Nbeats Oreshkin et al. (2020):** A neural approach for interpreting trend, seasonality, and residuals.

In an ablation study, we additionally compare against the following canonical denoising and boosting approaches for the Autoformer model. We obtain very similar results for the Informer model, omitted here but provided in Appendix A.

**AutoDWC (denoise without corruption):** a forecast-denoise model, where the denoising acts directly on the predictions (no blurring).

**AutoRB (residual-boosted):** two forecasting models, where the second is trained on minimizing the error residuals between the predictions and the ground-truth.

**AutoDT (denoise only during Training):** the forecasting model is trained to denoise with GP blurring, but the blurring is not used at test time.

<sup>3</sup>Solar energy <https://www.nrel.gov/grid/assets/downloads/al-pv-2006.zip>

<sup>4</sup>Electricity [https://archive.ics.uci.edu/ml/machine-learning-databases/00321/LD2011\\_2014.txt.zip](https://archive.ics.uci.edu/ml/machine-learning-databases/00321/LD2011_2014.txt.zip)

### 3.3 MODEL TRAINING AND HYPER-PARAMETERS

All models are trained and evaluated three times using three different random seeds. We use Optuna Akiba et al. (2019) for hyper-parameter optimization. We tune the warm up steps of the optimization, model size (dimensionality of latent space) for all models, chosen from  $\{16, 32\}$ , and the number of layers of the forecasting model chosen from  $\{1, 2\}$ .

We use 8-head attention for all attention-based models. We model the GP using ApproximateGP of the GPyTorch package.<sup>5</sup> The batch size is set to 256. We use the Adam Kingma & Ba (2015) optimizer with  $\beta_1 = 0.9$ ,  $\beta_2 = 0.98$  and  $\epsilon = 10^{-9}$ , we change the learning rate following Vaswani et al. (2017) with warm-up steps chosen from  $\{1000, 8000\}$ . All models are trained on a single NVIDIA A40 GPU with 45GB of memory. We train our forecasting and denoising model with total number of 50 epochs. Training one epoch of our end-to-end model roughly takes about 25 seconds.

### 3.4 RESULTS AND DISCUSSION

Table 1 and 2 summarize the evaluation results of the treatments of the Autoformer and Informer forecasting models along with other baselines on the three datasets. Results are reported as average and standard errors in terms of MSE. All forecasting models are evaluated on their ability to predict for the next 24, 48, 72 and 96 future time steps. When treating the Autoformer and Informer models, our proposed GP-based forecast-blur-denoise forecasting model predominately outperforms the Auto(Info)DI and the initial forecasting models. This finding is consistent across all data sets.

Next we conduct an ablation study by comparing our approach with several canonical denoising and boosting approaches. Table 3 presents an overview of the additional treatments applied to the Autoformer model. Compared to using a denoising approach during training (AutoDT), our model consistently performs better, supporting our claims. When attempting to denoise predictions directly without applying corruption, AutoDWC does not consistently yield improvements over the untreated forecasting model Autoformer. This highlights the significance of our GP blur model in enhancing the resilience and accuracy of the forecasts. This inconsistency in improving the untreated forecasting model is apparent in the AutoDI model as well. This reinforces our hypothesis that denoising isotropic noise does not provide benefits for time series data. This applies when dealing with time series forecasting model that do not exhibit jitters in their predictions.

The success of our forecast-blur-denoise model in comparison to traditional denoising models lies in the division of responsibilities arising from the GP blur model. As a result the initial forecasting model focuses on predicting the broader patterns and trends, while a dedicated denoising forecaster addresses the finer details. This results in an overall more accurate forecasting model.

Please refer to Appendix A for other extensive ablation studies, examples of actual forecasts, and other supplementary materials further supporting our claims.

## 4 SOCIETAL CONSEQUENCES

Time series forecasting offers societal benefits such as optimizing traffic lights, aligning energy grid capacities with solar power, and providing quantitative models for scientific understanding. However, like any foundational technology, it can also be misused for negative impacts, like aiding criminals or misinformation campaigns. By enhancing machine learning methods for more accurate forecasting, we aim to improve current practices, with the hope that the positive aspects will prevail.

## 5 CONCLUSION

In this paper, we study the multi-horizon time series forecasting problem and propose an end-to-end forecast-blur-denoise paradigm. In our proposed framework, we encourage the initial forecasting model to focus on accurately predicting the coarse-grained behavior, while the denoising model is responsible for predicting the fine-grained behavior. Both parts of the model communicate via a GP model, which will blur the predictions in order to be denoised, and hence encourage a separation

<sup>5</sup><https://gpytorch.ai/>

of concerns. This ultimately leads to more resilient forecasting methods. In addition to end-to-end training of the multi-component model, we utilize methods from variational techniques to guide the training of the denoising model via distribution matching.

Where most denoising methods leverage isotropic Gaussians, we hypothesize that a blur/noise model that generates smooth and correlated functions offers the most advantages in the time series domain. In line with Robinson et al. (2018), we find that using a noise model with temporal correlation, such as the Gaussian Process, is advantageous over uncorrelated noise models. Our experiments show that our proposed framework with Gaussian Process blurring is significantly outperforming the forecasting model without any denoising as well as denoising isotropic Gaussian noise. Additionally, we show that our forecast-blur-denoise framework predominately outperforms an approach that uses blurring/denoising only during training (AutoDT).

A strength of our approach is that it can be applied to any neural forecasting model. We demonstrate the effectiveness of our approach across three real-world datasets, different horizons, and several the-state-of-the-art forecasting models, including Autoformer and Informer. In all experiments, our proposed forecast-blur-denoise forecasting approach with Gaussian Process leads to significant improvements.

## REFERENCES

- Takuya Akiba, Shotaro Sano, Toshihiko Yanase, Takeru Ohta, and Masanori Koyama. Optuna: A next-generation hyperparameter optimization framework. In *Proceedings of the 25th ACM SIGKDD International Conference on Knowledge Discovery & Data Mining, KDD '19*, pp. 2623–2631, New York, NY, USA, 2019. Association for Computing Machinery. ISBN 9781450362016. doi: 10.1145/3292500.3330701. URL <https://doi.org/10.1145/3292500.3330701>.
- Carlos Capistrán, Christian Constandse, and Manuel Ramos-Francia. Multi-horizon inflation forecasts using disaggregated data. *Economic Modelling*, 27(3):666–677, May 2010. URL <https://ideas.repec.org/a/eee/ecmode/v27y2010i3p666-677.html>.
- Ankush Chakrabarty, Gordon Wichern, and Christopher Laughman. Attentive neural processes and batch bayesian optimization for scalable calibration of physics-informed digital twins. *arXiv preprint arXiv:2106.15502*, 2021.
- Ming-Fang Chang, John Lambert, Patsorn Sangkloy, Jagjeet Singh, Slawomir Bak, Andrew Hartnett, De Wang, Peter Carr, Simon Lucey, Deva Ramanan, and James Hays. Argoverse: 3d tracking and forecasting with rich maps. In *2019 IEEE/CVF Conference on Computer Vision and Pattern Recognition (CVPR)*, pp. 8740–8749, 2019. doi: 10.1109/CVPR.2019.00895.
- Kamil Deja, Anna Kuzina, Tomasz Trzcinski, and Jakub Mikolaj Tomczak. On analyzing generative and denoising capabilities of diffusion-based deep generative models. In Alice H. Oh, Alekh Agarwal, Danielle Belgrave, and Kyunghyun Cho (eds.), *Advances in Neural Information Processing Systems*, 2022. URL <https://openreview.net/forum?id=nx1-IjnDCRo>.
- Chenyou Fan, Yuze Zhang, Yi Pan, Xiaoyue Li, Chi Zhang, Rong Yuan, Di Wu, Wensheng Wang, Jian Pei, and Heng Huang. Multi-horizon time series forecasting with temporal attention learning. In *Proceedings of the 25th ACM SIGKDD International Conference on Knowledge Discovery & Data Mining, KDD '19*, pp. 2527–2535, New York, NY, USA, 2019. Association for Computing Machinery. ISBN 9781450362016. doi: 10.1145/3292500.3330662. URL <https://doi.org/10.1145/3292500.3330662>.
- James Hensman, Alexander Matthews, and Zoubin Ghahramani. Scalable Variational Gaussian Process Classification. In Guy Lebanon and S. V. N. Vishwanathan (eds.), *Proceedings of the Eighteenth International Conference on Artificial Intelligence and Statistics*, volume 38 of *Proceedings of Machine Learning Research*, pp. 351–360, San Diego, California, USA, 09–12 May 2015. PMLR. URL <https://proceedings.mlr.press/v38/hensman15.html>.
- Jonathan Ho, Ajay Jain, and Pieter Abbeel. Denoising diffusion probabilistic models. In H. Larochelle, M. Ranzato, R. Hadsell, M.F. Balcan, and H. Lin (eds.), *Advances in Neural Information Processing Systems*, volume 33, pp. 6840–6851. Curran Associates, Inc., 2020. URL <https://proceedings.neurips.cc/paper/2020/file/4c5bcfec8584af0d967f1ab10179ca4b-Paper.pdf>.

- Sepp Hochreiter and Jürgen Schmidhuber. Long short-term memory. *Neural computation*, 9:1735–80, 12 1997. doi: 10.1162/neco.1997.9.8.1735.
- Rob J. Hyndman and Yeasmin Khandakar. Automatic time series forecasting: The forecast package for r. *Journal of Statistical Software*, 27(3):1–22, 2008. doi: 10.18637/jss.v027.i03. URL <https://www.jstatsoft.org/index.php/jss/article/view/v027i03>.
- Urvashi Khandelwal, He He, Peng Qi, and Dan Jurafsky. Sharp nearby, fuzzy far away: How neural language models use context. In *Proceedings of the 56th Annual Meeting of the Association for Computational Linguistics (Volume 1: Long Papers)*, pp. 284–294, Melbourne, Australia, July 2018. Association for Computational Linguistics. doi: 10.18653/v1/P18-1027. URL <https://aclanthology.org/P18-1027>.
- Diederik P. Kingma and Jimmy Ba. Adam: A method for stochastic optimization. *CoRR*, abs/1412.6980, 2015.
- Sepideh Koohfar and Laura Dietz. An adaptive temporal attention mechanism to address distribution shifts. In *NeurIPS 2022 Workshop on Robustness in Sequence Modeling, 2022*. URL <https://openreview.net/forum?id=5aIwxkn0MzC>.
- Shiyang Li, Xiaoyong Jin, Yao Xuan, Xiyou Zhou, Wenhui Chen, Yu-Xiang Wang, and Xifeng Yan. *Enhancing the Locality and Breaking the Memory Bottleneck of Transformer on Time Series Forecasting*. Curran Associates Inc., Red Hook, NY, USA, 2019.
- Yan Li, Xinjiang Lu, Yaqing Wang, and Dejing Dou. Generative time series forecasting with diffusion, denoise, and disentanglement. In Alice H. Oh, Alekh Agarwal, Danielle Belgrave, and Kyunghyun Cho (eds.), *Advances in Neural Information Processing Systems, 2022*. URL <https://openreview.net/forum?id=rG0jm74xtx>.
- Bryan Lim. Forecasting treatment responses over time using recurrent marginal structural networks. In S. Bengio, H. Wallach, H. Larochelle, K. Grauman, N. Cesa-Bianchi, and R. Garnett (eds.), *Advances in Neural Information Processing Systems*, volume 31. Curran Associates, Inc., 2018. URL <https://proceedings.neurips.cc/paper/2018/file/56e6a93212e4482d99c84a639d254b67-Paper.pdf>.
- Alexander Quinn Nichol and Prafulla Dhariwal. Improved denoising diffusion probabilistic models. In *International Conference on Machine Learning*, pp. 8162–8171. PMLR, 2021.
- Boris N. Oreshkin, Dmitri Carпов, Nicolas Chapados, and Yoshua Bengio. N-beats: Neural basis expansion analysis for interpretable time series forecasting. In *International Conference on Learning Representations, 2020*. URL <https://openreview.net/forum?id=r1ecqn4YwB>.
- Kashif Rasul, Calvin Seward, Ingmar Schuster, and Roland Vollgraf. Autoregressive denoising diffusion models for multivariate probabilistic time series forecasting. In *International Conference on Machine Learning, 2021*.
- Danielle Robinson, Bernie Wang, and Alex Smola. Deep factors with gaussian processes for forecasting. In *NeurIPS 2018, 2018*. URL <https://www.amazon.science/publications/deep-factors-with-gaussian-processes-for-forecasting>.
- David Salinas, Valentin Flunkert, Jan Gasthaus, and Tim Januschowski. Deepar: Probabilistic forecasting with autoregressive recurrent networks. *International Journal of Forecasting*, 36(3):1181–1191, 2020. ISSN 0169-2070. doi: <https://doi.org/10.1016/j.ijforecast.2019.07.001>. URL <https://www.sciencedirect.com/science/article/pii/S0169207019301888>.
- Ashish Vaswani, Noam Shazeer, Niki Parmar, Jakob Uszkoreit, Llion Jones, Aidan N Gomez, Łukasz Kaiser, and Illia Polosukhin. Attention is all you need. In I. Guyon, U. V. Luxburg, S. Bengio, H. Wallach, R. Fergus, S. Vishwanathan, and R. Garnett (eds.), *Advances in Neural Information Processing Systems*, volume 30. Curran Associates, Inc., 2017. URL <https://proceedings.neurips.cc/paper/2017/file/3f5ee243547dee91fbd053c1c4a845aa-Paper.pdf>.

Pascal Vincent, Hugo Larochelle, Isabelle Lajoie, Yoshua Bengio, and Pierre-Antoine Manzagol. Stacked denoising autoencoders: Learning useful representations in a deep network with a local denoising criterion. *J. Mach. Learn. Res.*, 11:3371–3408, dec 2010. ISSN 1532-4435.

haixu Wu, Jiehui Xu, Jianmin Wang, and Mingsheng Long. Autoformer: Decomposition transformers with auto-correlation for long-term series forecasting. In M. Ranzato, A. Beygelzimer, Y. Dauphin, P.S. Liang, and J. Wortman Vaughan (eds.), *Advances in Neural Information Processing Systems*, volume 34, pp. 22419–22430. Curran Associates, Inc., 2021. URL <https://proceedings.neurips.cc/paper/2021/file/bcc0d400288793e8bdcd7c19a8ac0c2b-Paper.pdf>.

Ailing Zeng, Muxi Chen, Lei Zhang, and Qiang Xu. Are transformers effective for time series forecasting? In *Proceedings of the Thirty-Seventh AAAI Conference on Artificial Intelligence and Thirty-Fifth Conference on Innovative Applications of Artificial Intelligence and Thirteenth Symposium on Educational Advances in Artificial Intelligence, AAAI’23/IAAI’23/EAAI’23*. AAAI Press, 2023. ISBN 978-1-57735-880-0. doi: 10.1609/aaai.v37i9.26317. URL <https://doi.org/10.1609/aaai.v37i9.26317>.

Haoyi Zhou, Shanghang Zhang, Jieqi Peng, Shuai Zhang, Jianxin Li, Hui Xiong, and Wan Zhang. Informer: Beyond efficient transformer for long sequence time-series forecasting. In *AAAI*, 2021.

## A APPENDIX

**Actual Forecasts:** Please refer to Figure 3, 4, and 5 for the predicted forecasts of 72 future time steps for four treatments of Autoformer model including a) standalone forecasting b) AutoDI, c) AutoDWC, and d) AutoDG(ours) on Traffic, Electricity, and Solar datasets respectively .

**Convergence Plots:** Please refer to Figure 6, 7, and 8 for the convergence plots of three treatments of the Autoformer model including ours respectively.

**Main results of MAE metric:** Please refer to Table 4 and 6 for main results of MAE metric respectively.

**Ablation results of other denoising/boosting baselines:** Please refer to Table 5, 9, and 10 for the ablation results of Autoformer (MAE) and Informer (MSE and MAE) ablation studies on other denoising/boosting baselines respectively.

**Ablation results for higher number of layers (parameters) of the stand-alone forecasting models:** Please refer to Table 7 and 8 for the ablation study of higher number of layers (parameters) of stand-alone forecasting models respectively.

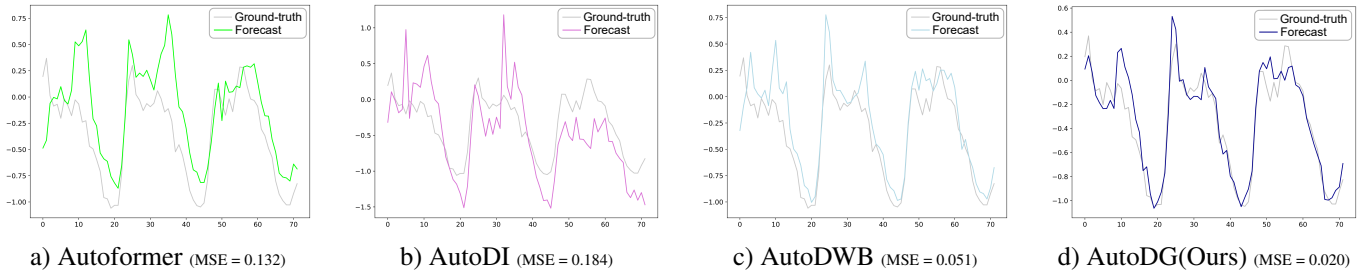


Figure 3: Example forecast of four treatments on the **Traffic** dataset for 72 future time steps using the Autoformer forecasting model. The values are plotted in Z-score normalized space. Standalone Autoformer model a) generally tracks the ground-truth, albeit fine-grained features are not accurately reproduced. Autoformer with isotropic noise and denoising (AutoDI) b) yields a higher MSE with forecasts containing many jitters leading to inaccurate local behavior. Denoising without blurring (AutoDWB) c) yield a better MSE but fine-grained features including details and extreme values are not accurately reproduced. Our proposed model with GP blurring and denoising (AutoDG) d) produces the most accurate forecasts by accurately predicting coarse-grained behavior of peaks and valleys, as well as fine-grained behavior such as smooth slopes, details and better extreme values prediction.

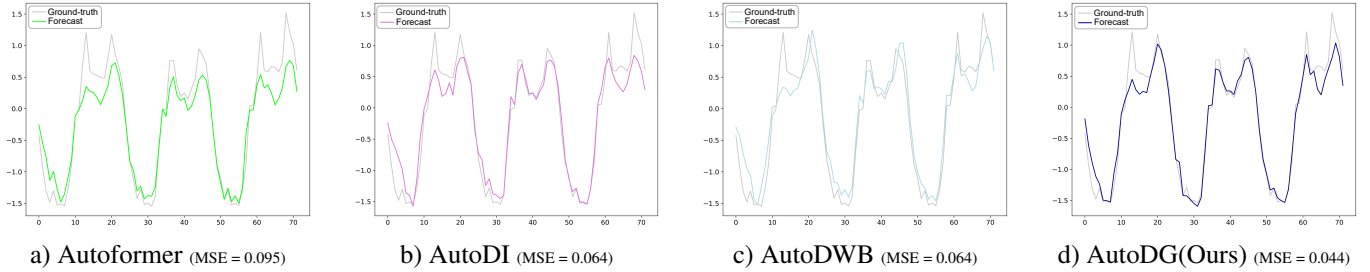


Figure 4: Example forecast of four treatments on the **Electricity** dataset for 72 future time steps using the Autoformer forecasting model. The values are plotted in Z-score normalized space. Standalone Autoformer model a) generally tracks the ground-truth, albeit fine-grained features are only roughly reproduced. Autoformer with isotropic noise and denoising (AutoDI) b) yields a lower MSE with fine-grained features being more accurately predicted. Denoising without blurring (AutoDWB) c) yields a better MSE compared to Autoformer a), however fine-grained features are less accurately predicted than AutoDI. Our proposed model with GP blurring and denoising (AutoDG) d) produces the most accurate forecasts by accurately predicting coarse-grained behavior of peaks and valleys, as well as fine-grained behavior such as smooth slopes, details and better extreme values prediction.

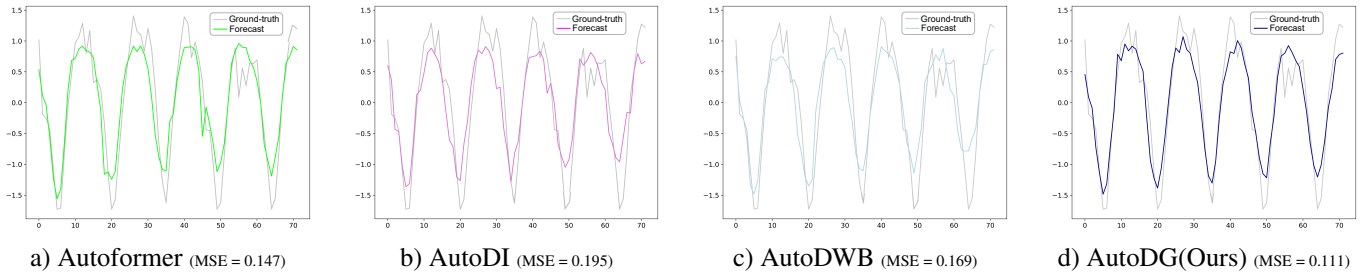


Figure 5: Example forecast of four treatments on the **Solar** dataset for 72 future time steps using the Autoformer forecasting model. The values are plotted in Z-score normalized space. Standalone Autoformer model a) generally tracks the ground-truth, albeit fine-grained features are only roughly reproduced. Autoformer with isotropic noise and denoising b) yields a higher MSE with less accurate local behavior (e.g. prediction of extreme values). Denoising without blurring (AutoDWB) c) yields a higher MSE than Autoformer a) with fine-grained features being less accurately predicted. Our proposed model with GP blurring and denoising (AutoDG) d) produces the most accurate forecasts by accurately predicting coarse-grained behavior of peaks and valleys, as well as fine-grained behavior such as smooth slopes, details and better extreme values prediction.

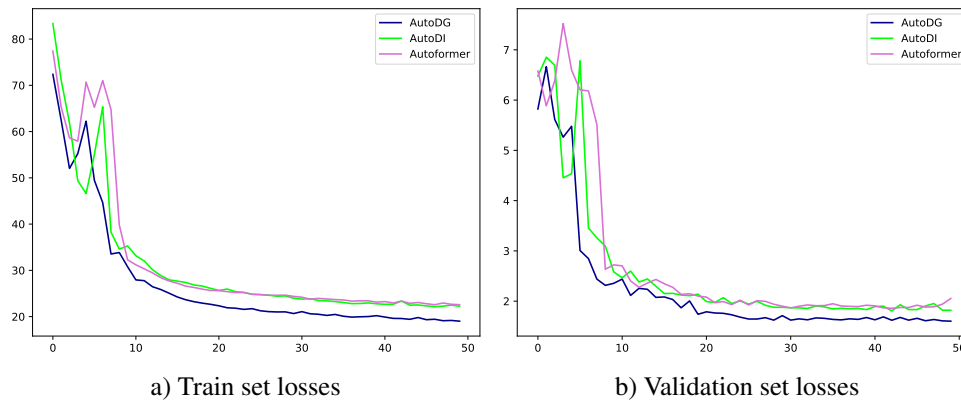


Figure 6: MSE loss illustration of Autformer, AutoDI, and AutoDG (Ours) of train a) and validation b) sets during training with 50 epochs on **Traffic** dataset when predicting for 72 future time steps. The plots demonstrate that our model offers a more favorable optimization space, showcasing superior convergence and absence of overfitting when compared to Autformer and AutoDI approaches.

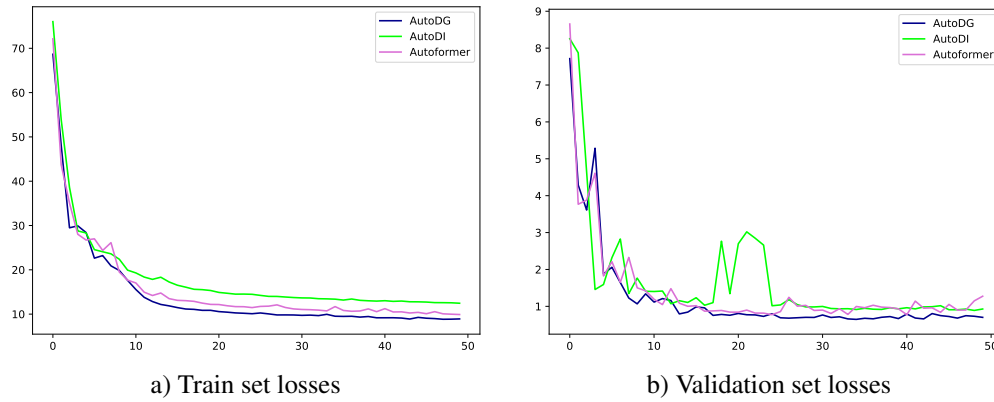


Figure 7: MSE loss illustration of Autformer, AutoDI, and AutoDG (Ours) of train a) and validation b) sets during training with 50 epochs on **Electricity** dataset when predicting for 72 future time steps. The plots demonstrate that our model offers a more favorable optimization space, showcasing superior convergence and absence of overfitting when compared to Autformer and AutoDI approaches.

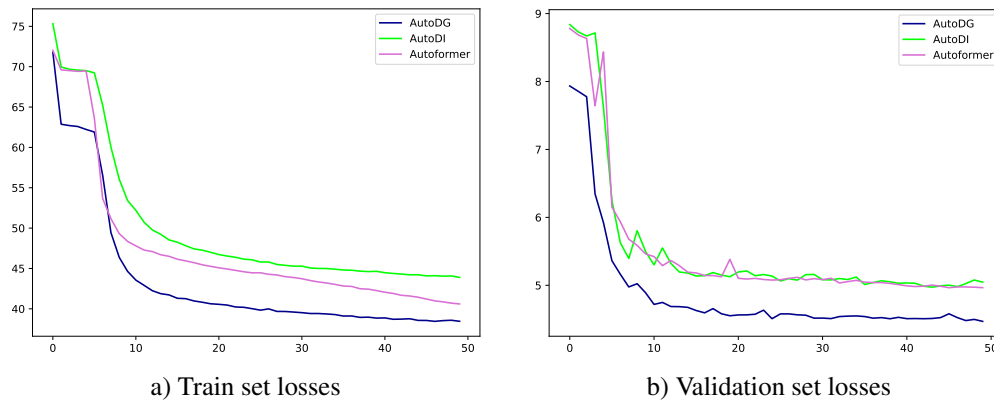


Figure 8: MSE loss illustration of Autformer, AutoDI, and AutoDG (Ours) of train a) and validation b) sets during training with 50 epochs on **Solar** dataset when predicting for 72 future time steps. The plots demonstrate that our model offers a more favorable optimization space, showcasing superior convergence and absence of overfitting when compared to Autformer and AutoDI approaches.

Table 4: Overall results of the quantitative evaluation of our forecast-blur-denoise and other baseline models in terms of average and standard error of **MAE**. We compare the forecasting models on all three datasets with different number of forecasting steps. A lower **MAE** indicates a better model. Our forecast-blur-denoise approach with GPs improves performance of the original forecasting model (Autoformer) and isotropic Gaussian noise model (AutoDI). (Note that to provide a fair comparison, all the baseline models considered in this study were trained and evaluated under the *same* experimental setup as our proposed model. Consequently, the reported results may differ from those originally reported in the respective baseline papers. We provide the baseline models in our online repository).

Dataset	Horizon	<b>AutoDG(Ours)</b>	Autoformer	AutoDI	NBeats	DLinear	DeepAR	CMGP	ARIMA
Traffic	24	<b>0.333</b> ±0.010	<b>0.334</b> ±0.007	<b>0.340</b> ±0.007	0.384 ±0.001	0.447 ±0.000	0.652 ±0.000	0.645 ±0.000	0.770 ±0.000
	48	<b>0.328</b> ±0.001	0.368 ±0.006	0.343 ±0.006	0.408 ±0.003	0.462 ±0.000	0.650 ±0.000	0.642 ±0.000	0.776 ±0.000
	72	<b>0.358</b> ±0.013	<b>0.356</b> ±0.003	<b>0.356</b> ±0.005	0.413 ±0.004	0.466 ±0.000	0.636 ±0.000	0.648 ±0.000	0.782 ±0.000
	96	<b>0.333</b> ±0.000	0.359 ±0.004	0.366 ±0.004	0.414 ±0.002	0.471 ±0.000	0.632 ±0.000	0.647 ±0.000	0.773 ±0.000
Electricity	24	<b>0.249</b> ±0.001	0.265 ±0.003	0.258 ±0.001	0.294 ±0.004	0.299 ±0.000	0.862 ±0.000	0.840 ±0.000	0.959 ±0.000
	48	<b>0.275</b> ±0.003	0.292 ±0.007	0.301 ±0.003	0.310 ±0.007	0.308 ±0.000	0.853 ±0.000	0.839 ±0.000	0.971 ±0.000
	72	<b>0.303</b> ±0.004	<b>0.297</b> ±0.006	<b>0.303</b> ±0.004	0.322 ±0.007	0.323 ±0.000	0.856 ±0.000	0.836 ±0.000	0.987 ±0.000
	96	<b>0.304</b> ±0.001	0.372 ±0.010	0.325 ±0.002	0.324 ±0.002	0.329 ±0.000	0.850 ±0.000	0.832 ±0.000	0.983 ±0.000
Solar	24	<b>0.548</b> ±0.009	0.603 ±0.002	0.574 ±0.008	0.632 ±0.001	0.801 ±0.000	0.885 ±0.000	0.885 ±0.000	1.100 ±0.000
	48	<b>0.612</b> ±0.003	0.656 ±0.003	0.638 ±0.003	0.710 ±0.001	0.864 ±0.000	0.865 ±0.000	0.888 ±0.000	1.102 ±0.000
	72	<b>0.702</b> ±0.0001	0.729 ±0.017	<b>0.702</b> ±0.001	0.744 ±0.001	0.894 ±0.000	0.873 ±0.000	0.885 ±0.000	1.106 ±0.000
	96	<b>0.725</b> ±0.000	0.754 ±0.009	0.747 ±0.005	0.781 ±0.002	0.911 ±0.000	0.866 ±0.000	0.882 ±0.000	1.097 ±0.000

Table 5: Comparison of different denoising baselines to our forecast-blur-denoise approach with GPs when treating Autoformer forecasting model. We find that our approach predominantly outperforms the other denoising approaches. Results are reported as average and standard error of **MAE**. A lower **MAE** indicates a better forecasting model.

Dataset	Horizon	<b>AutoDG(Ours)</b>	Autoformer	AutoDI	AutoDWC	AutoRB	AutoDT
Traffic	24	<b>0.333</b> ±0.010	<b>0.334</b> ±0.007	<b>0.340</b> ±0.007	0.345±0.009	0.391±0.005	0.349±0.005
	48	<b>0.328</b> ±0.001	0.368±0.006	0.343±0.006	0.351±0.005	0.359±0.002	0.361±0.016
	72	<b>0.358</b> ±0.013	<b>0.356</b> ±0.003	<b>0.356</b> ±0.005	0.361±0.002	0.383±0.005	0.379±0.001
	96	<b>0.304</b> ±0.000	0.325±0.004	0.372±0.004	0.362±0.004	0.368±0.005	0.379±0.005
Electricity	24	<b>0.249</b> ±0.001	0.265±0.003	0.258±0.001	0.272±0.001	0.380±0.001	0.263±0.007
	48	<b>0.275</b> ±0.003	0.292±0.007	0.301±0.003	0.306±0.002	0.311±0.002	0.288±0.003
	72	<b>0.303</b> ±0.004	<b>0.297</b> ±0.006	<b>0.303</b> ±0.004	<b>0.295</b> ±0.009	0.330±0.021	<b>0.305</b> ±0.003
	96	<b>0.304</b> ±0.001	0.372±0.010	0.325±0.002	0.324±0.005	0.386±0.005	0.318±0.005
Solar	24	<b>0.548</b> ±0.009	0.603±0.002	0.574±0.008	0.549±0.008	0.601±0.005	0.598±0.006
	48	<b>0.612</b> ±0.003	0.656±0.003	0.638±0.003	0.656±0.002	0.645±0.003	0.655±0.003
	72	<b>0.702</b> ±0.001	0.729±0.017	<b>0.702</b> ±0.001	0.724±0.008	0.720±0.010	0.709±0.004
	96	<b>0.725</b> ±0.000	0.754±0.009	0.747±0.005	0.746±0.006	0.738±0.007	0.745±0.006

Table 6: Overall results of the quantitative evaluation of our forecast-blur-denoise model in terms of average and standard error of **MAE**. We compare the forecasting models on all three datasets with different number of forecasting steps. A lower **MAE** indicates a better model. Our forecast-blur-denoise approach with GPs predominantly improves the performance of the original forecasting model (Informer) and isotropic Gaussian noise model (InfoDI). (Note that to provide a fair comparison, all the baseline models considered in this study were trained and evaluated under the *same* experimental setup as our proposed model. Consequently, the reported results may differ from those originally reported in the respective baseline papers. We provide the baseline models in our online repository).

Dataset	Horizon	InfoDG(Ours)	Informer	InfoDI	NBeats	DLinear	DeepAR	CMGP	ARIMA
Traffic	24	0.355 ±0.007	<b>0.329</b> ±0.006	0.342 ±0.004	0.384 ±0.001	0.447 ±0.000	0.652 ±0.000	0.645 ±0.000	0.770 ±0.000
	48	<b>0.350</b> ±0.001	<b>0.354</b> ±0.012	<b>0.362</b> ±0.005	0.408 ±0.003	0.462 ±0.000	0.650 ±0.000	0.642 ±0.000	0.776 ±0.000
	72	<b>0.345</b> ±0.003	0.377 ±0.002	0.353 ±0.008	0.413 ±0.004	0.466 ±0.000	0.636 ±0.000	0.648 ±0.000	0.782 ±0.000
	96	<b>0.397</b> ±0.004	<b>0.402</b> ±0.011	<b>0.402</b> ±0.005	<b>0.414</b> ±0.002	0.471 ±0.000	0.632 ±0.000	0.647 ±0.000	0.773 ±0.000
Electricity	24	<b>0.290</b> ±0.008	<b>0.300</b> ±0.005	<b>0.298</b> ±0.003	<b>0.294</b> ±0.004	<b>0.299</b> ±0.000	0.862 ±0.000	0.840 ±0.000	0.959 ±0.000
	48	<b>0.311</b> ±0.002	0.349 ±0.009	0.325 ±0.002	0.310 ±0.007	0.308 ±0.000	0.853 ±0.000	0.839 ±0.000	0.971 ±0.000
	72	<b>0.345</b> ±0.003	0.377 ±0.002	0.353 ±0.008	0.322 ±0.002	0.323 ±0.000	0.856 ±0.000	0.836 ±0.000	0.987 ±0.000
	96	<b>0.342</b> ±0.004	0.378 ±0.011	0.379 ±0.005	0.324 ±0.002	0.329 ±0.000	0.850 ±0.000	0.832 ±0.000	0.983 ±0.000
Solar	24	<b>0.533</b> ±0.005	0.597 ±0.002	0.563 ±0.003	0.632 ±0.001	0.801 ±0.000	0.885 ±0.000	0.885 ±0.000	1.100 ±0.000
	48	<b>0.624</b> ±0.007	0.681 ±0.013	0.635 ±0.005	0.710 ±0.001	0.864 ±0.000	0.865 ±0.000	0.888 ±0.000	1.102 ±0.000
	72	<b>0.690</b> ±0.013	0.752 ±0.017	0.735 ±0.019	0.744 ±0.001	0.894 ±0.000	0.873 ±0.000	0.885 ±0.000	1.106 ±0.000
	96	<b>0.727</b> ±0.006	0.772 ±0.012	0.764 ±0.004	0.781 ±0.002	0.911 ±0.000	0.866 ±0.000	0.882 ±0.000	1.097 ±0.000

Table 7: Comparison of our forecast-blur-denoise approach with standalone forecasting models with higher number of layers (parameters) denoted by † sign. Initially, the number of layers for our proposed model and other baselines are chosen from {1, 2}, however to show that the performance of our model is indeed stems from its mechanism, we included the results of stand-alone forecasting models with number of layers chosen from {3, 4}. Results are reported as average and standard error of **MSE**. A lower **MSE** indicates a better forecasting model.

Dataset	Horizon	<b>AutoDG(Ours)</b>	Autoformer	Autoformer <sup>†</sup>	<b>InfoDG(Ours)</b>	Informer	Informer <sup>†</sup>
Traffic	24	0.392 ±0.006	0.412 ±0.006	<b>0.359</b> ±0.007	<b>0.398</b> ±0.006	0.421 ±0.006	0.422 ±0.009
	48	0.387 ±0.001	0.422 ±0.007	<b>0.383</b> ±0.001	<b>0.399</b> ±0.001	0.434 ±0.001	0.486 ±0.010
	72	<b>0.380</b> ±0.001	<b>0.383</b> ±0.002	0.442 ±0.006	<b>0.380</b> ±0.001	0.436 ±0.001	0.412 ±0.003
	96	<b>0.385</b> ±0.003	0.400 ±0.004	0.416 ±0.001	<b>0.397</b> ±0.003	<b>0.402</b> ±0.003	0.408 ±0.005
Electricity	24	<b>0.165</b> ±0.001	0.187 ±0.003	0.242 ±0.007	<b>0.193</b> ±0.001	0.222 ±0.001	0.266 ±0.001
	48	<b>0.188</b> ±0.003	0.203 ±0.008	0.232 ±0.005	<b>0.222</b> ±0.002	0.262 ±0.002	0.293 ±0.002
	72	<b>0.209</b> ±0.004	0.230 ±0.001	0.263 ±0.004	<b>0.238</b> ±0.001	0.280 ±0.003	0.310 ±0.002
	96	<b>0.211</b> ±0.001	0.230 ±0.014	0.224 ±0.004	<b>0.242</b> ±0.001	0.289 ±0.002	0.327 ±0.003
Solar	24	<b>0.446</b> ±0.002	0.472 ±0.003	0.524 ±0.001	<b>0.455</b> ±0.009	0.524 ±0.003	0.498 ±0.001
	48	<b>0.546</b> ±0.005	0.603 ±0.003	0.622 ±0.001	<b>0.556</b> ±0.005	0.629 ±0.003	0.690 ±0.031
	72	<b>0.666</b> ±0.003	<b>0.667</b> ±0.004	0.701 ±0.004	<b>0.643</b> ±0.003	0.729 ±0.023	0.716 ±0.024
	96	<b>0.713</b> ±0.004	0.739 ±0.009	0.744 ±0.002	<b>0.708</b> ±0.004	0.770 ±0.004	0.738 ±0.002

Table 8: Comparison of our forecast-blur-denoise with standalone forecasting models with higher number of layers (parameters) denoted by † sign. Initially, the number of layers for our proposed model and other baselines are chosen from {1, 2}, however to show that the performance of our model is indeed stems from its mechanism, we included the results of stand-alone forecasting models with number of layers chosen from {3, 4}. Results are reported as average and standard error of **MAE**. A lower **MAE** indicates a better forecasting model.

Dataset	Horizon	<b>AutoDG(Ours)</b>	Autoformer	Autoformer <sup>†</sup>	<b>InfoDG(Ours)</b>	Informer	Informer <sup>†</sup>
Traffic	24	<b>0.333</b> ±0.010	<b>0.334</b> ±0.007	<b>0.332</b> ±0.002	0.355 ±0.007	<b>0.329</b> ±0.006	0.382 ±0.003
	48	<b>0.328</b> ±0.001	0.368 ±0.002	0.336 ±0.001	<b>0.345</b> ±0.001	0.377 ±0.013	0.402 ±0.005
	72	<b>0.358</b> ±0.013	<b>0.356</b> ±0.003	0.357 ±0.001	<b>0.345</b> ±0.003	0.377 ±0.010	0.382 ±0.011
	96	<b>0.385</b> ±0.003	0.400 ±0.004	0.370 ±0.001	<b>0.397</b> ±0.003	<b>0.402</b> ±0.002	0.413 ±0.003
Electricity	24	<b>0.249</b> ±0.001	0.265 ±0.003	0.303 ±0.003	<b>0.290</b> ±0.003	<b>0.300</b> ±0.006	0.332 ±0.002
	48	<b>0.275</b> ±0.001	0.292 ±0.007	0.317 ±0.002	<b>0.311</b> ±0.002	0.349 ±0.009	0.377 ±0.002
	72	<b>0.303</b> ±0.004	<b>0.297</b> ±0.007	0.351 ±0.002	<b>0.336</b> ±0.003	0.371 ±0.002	0.384 ±0.002
	96	<b>0.304</b> ±0.001	0.372 ±0.010	0.317 ±0.001	<b>0.342</b> ±0.004	0.378 ±0.001	0.411 ±0.003
Solar	24	<b>0.548</b> ±0.009	0.603 ±0.002	0.608 ±0.001	<b>0.533</b> ±0.005	0.597 ±0.002	0.575 ±0.000
	48	<b>0.612</b> ±0.003	0.656 ±0.003	0.672 ±0.004	<b>0.624</b> ±0.007	0.681 ±0.013	0.745 ±0.020
	72	<b>0.702</b> ±0.001	0.729 ±0.017	0.707 ±0.001	<b>0.690</b> ±0.013	0.752 ±0.017	0.762 ±0.016
	96	<b>0.725</b> ±0.000	0.754 ±0.009	0.737 ±0.002	<b>0.727</b> ±0.006	0.772 ±0.012	0.785 ±0.010

Table 9: Comparison of different denoising baselines to our forecast-blur-denoise approach with GPs when treating Informer forecasting model. We find that our approach predominantly outperforms the other denoising approaches. Results are reported as average and standard error of **MSE**. A lower **MSE** indicates a better forecasting model.

Dataset	Horizon	InfoDG(Ours)	Informer	InfoDI	InfoDWC	InfoRB	InfoDT
Traffic	24	<b>0.398</b> $\pm$ 0.005	0.421 $\pm$ 0.005	0.415 $\pm$ 0.002	0.406 $\pm$ 0.002	0.435 $\pm$ 0.005	0.473 $\pm$ 0.003
	48	<b>0.399</b> $\pm$ 0.004	0.434 $\pm$ 0.014	0.395 $\pm$ 0.007	0.392 $\pm$ 0.003	<b>0.395</b> $\pm$ 0.011	0.421 $\pm$ 0.014
	72	<b>0.380</b> $\pm$ 0.001	0.436 $\pm$ 0.015	0.395 $\pm$ 0.001	0.392 $\pm$ 0.001	0.407 $\pm$ 0.009	0.421 $\pm$ 0.011
	96	<b>0.397</b> $\pm$ 0.003	0.402 $\pm$ 0.002	<b>0.402</b> $\pm$ 0.006	<b>0.394</b> $\pm$ 0.003	0.412 $\pm$ 0.007	0.414 $\pm$ 0.015
Electricity	24	<b>0.193</b> $\pm$ 0.003	0.222 $\pm$ 0.006	0.212 $\pm$ 0.001	0.204 $\pm$ 0.005	0.225 $\pm$ 0.009	0.230 $\pm$ 0.007
	48	<b>0.222</b> $\pm$ 0.003	0.262 $\pm$ 0.013	0.229 $\pm$ 0.003	0.241 $\pm$ 0.007	0.261 $\pm$ 0.014	0.256 $\pm$ 0.004
	72	<b>0.238</b> $\pm$ 0.001	0.280 $\pm$ 0.006	0.253 $\pm$ 0.006	0.263 $\pm$ 0.013	0.262 $\pm$ 0.008	0.268 $\pm$ 0.008
	96	<b>0.242</b> $\pm$ 0.004	0.289 $\pm$ 0.011	0.275 $\pm$ 0.005	0.279 $\pm$ 0.006	0.283 $\pm$ 0.001	0.275 $\pm$ 0.007
Solar	24	<b>0.455</b> $\pm$ 0.007	0.524 $\pm$ 0.002	0.465 $\pm$ 0.006	0.457 $\pm$ 0.006	0.498 $\pm$ 0.010	0.512 $\pm$ 0.012
	48	<b>0.556</b> $\pm$ 0.011	0.629 $\pm$ 0.021	0.570 $\pm$ 0.007	0.590 $\pm$ 0.016	0.623 $\pm$ 0.016	0.629 $\pm$ 0.023
	72	<b>0.643</b> $\pm$ 0.022	0.729 $\pm$ 0.024	0.707 $\pm$ 0.026	0.708 $\pm$ 0.014	0.748 $\pm$ 0.010	0.726 $\pm$ 0.006
	96	<b>0.708</b> $\pm$ 0.010	0.770 $\pm$ 0.017	0.766 $\pm$ 0.006	0.739 $\pm$ 0.010	0.781 $\pm$ 0.017	0.777 $\pm$ 0.000

Table 10: Comparison of different denoising baselines to our forecast-blur-denoise approach with GPs when treating Informer forecasting model. We find that our approach predominantly outperforms the other denoising approaches. Results are reported as average and standard error of **MAE**. A lower **MAE** indicates a better forecasting model.

Dataset	Horizon	InfoDG(Ours)	Informer	InfoDI	InfoDWC	InfoRB	InfoDT
Traffic	24	0.355 $\pm$ 0.007	<b>0.329</b> $\pm$ 0.006	0.342 $\pm$ 0.004	0.337 $\pm$ 0.003	0.331 $\pm$ 0.003	0.379 $\pm$ 0.003
	48	<b>0.345</b> $\pm$ 0.001	0.377 $\pm$ 0.013	0.353 $\pm$ 0.005	0.348 $\pm$ 0.003	0.353 $\pm$ 0.009	0.375 $\pm$ 0.006
	72	<b>0.345</b> $\pm$ 0.003	0.377 $\pm$ 0.010	0.353 $\pm$ 0.004	0.348 $\pm$ 0.001	0.379 $\pm$ 0.005	0.361 $\pm$ 0.006
	96	<b>0.350</b> $\pm$ 0.004	<b>0.354</b> $\pm$ 0.006	<b>0.362</b> $\pm$ 0.007	<b>0.348</b> $\pm$ 0.008	0.379 $\pm$ 0.005	<b>0.361</b> $\pm$ 0.011
Electricity	24	<b>0.290</b> $\pm$ 0.008	<b>0.300</b> $\pm$ 0.005	<b>0.298</b> $\pm$ 0.003	<b>0.295</b> $\pm$ 0.004	<b>0.302</b> $\pm$ 0.009	0.318 $\pm$ 0.003
	48	<b>0.311</b> $\pm$ 0.002	0.349 $\pm$ 0.009	0.325 $\pm$ 0.002	0.333 $\pm$ 0.004	0.343 $\pm$ 0.009	0.343 $\pm$ 0.005
	72	<b>0.336</b> $\pm$ 0.003	0.371 $\pm$ 0.002	0.359 $\pm$ 0.008	0.362 $\pm$ 0.008	0.359 $\pm$ 0.006	0.367 $\pm$ 0.008
	96	<b>0.342</b> $\pm$ 0.004	0.378 $\pm$ 0.0011	0.379 $\pm$ 0.005	0.384 $\pm$ 0.006	0.375 $\pm$ 0.001	0.370 $\pm$ 0.007
Solar	24	<b>0.533</b> $\pm$ 0.005	0.597 $\pm$ 0.002	0.563 $\pm$ 0.003	0.551 $\pm$ 0.001	0.573 $\pm$ 0.008	0.596 $\pm$ 0.007
	48	<b>0.624</b> $\pm$ 0.007	0.681 $\pm$ 0.013	0.635 $\pm$ 0.005	0.649 $\pm$ 0.011	0.675 $\pm$ 0.012	0.681 $\pm$ 0.012
	72	<b>0.690</b> $\pm$ 0.013	0.752 $\pm$ 0.017	0.735 $\pm$ 0.019	0.736 $\pm$ 0.011	0.763 $\pm$ 0.020	0.735 $\pm$ 0.004
	96	<b>0.727</b> $\pm$ 0.006	0.772 $\pm$ 0.012	0.764 $\pm$ 0.004	0.753 $\pm$ 0.005	0.777 $\pm$ 0.014	0.766 $\pm$ 0.002